



Published in final edited form as:

*Environ Sci Nano*. 2018 June 1; 5(6): 1473–1481. doi:10.1039/C8EN00055G.

## Reactive oxygen species generation is likely a driver of copper based nanomaterial toxicity

Lindsay Denluck<sup>a</sup>, Fan Wu<sup>b</sup>, Lauren E. Crandon<sup>b</sup>, Bryan J. Harper<sup>a</sup>, and Stacey L. Harper<sup>†,a,b,c</sup>

<sup>a</sup>Department of Environmental and Molecular Toxicology, Oregon State University, Corvallis OR, USA

<sup>b</sup>School of Chemical, Biological, and Environmental Engineering, Oregon State University, Corvallis OR, USA

<sup>c</sup>Oregon Nanoscience and Microtechnologies Institute, Eugene OR, USA

### Abstract

Determining the specific nanomaterial features that elicit adverse biological responses is important to inform risk assessments, develop targeted applications, and rationally design future nanomaterials. Embryonic zebrafish are often employed to study nanomaterial-biological interactions, but few studies address the role of the chorion in nanomaterial exposure and toxicity. Here, we used chorion-intact (CI) or dechorionated (DC) embryonic zebrafish to investigate the influence of the chorion on copper-based nanoparticle toxicity. We found that despite higher dissolution and uptake, CuO NPs were less toxic than Cu NPs regardless of chorion status and did not cause 100 % mortality at even the highest exposure concentration. The presence of the chorion inhibited Cu toxicity: DC exposures to Cu NPs had an LC<sub>50</sub> of 2.5 ± 0.3 mg/L compared to a CI LC<sub>50</sub> of 13.7 ± 0.8 mg/L. This highlights the importance of considering zebrafish chorion status during nanotoxicological investigations, as embryo sensitivity increased by one order of magnitude or more when chorions were removed. Agglomerate size, zeta potential, and dissolved Cu did not sufficiently explain the differences in toxicity between Cu NPs and CuO NPs; however, reactive oxygen species (ROS) generation did. Cu NPs generated ROS in a concentration-dependent manner, while CuO did not and generated less than Cu NPs. We believe that the differences between the toxicities of Cu NPs and CuO NPs are due in part to their ability to generate ROS which could and should be a hazard consideration for risk assessments.

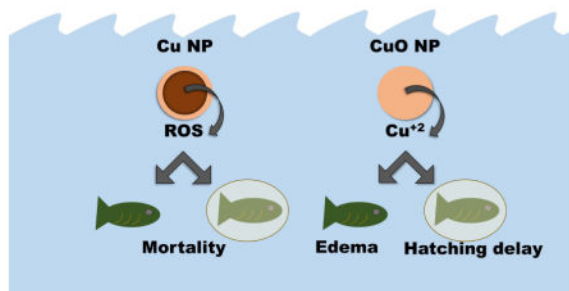
### Graphical Abstract

<sup>†</sup>Corresponding author: stacey.harper@oregonstate.edu.

<sup>†</sup>Electronic Supplementary Information (ESI) available: [details of any supplementary information available should be included here]. See DOI: 10.1039/b000000x/

#### Conflict of Interest

There are no conflicts of interest to declare.



## Introduction

Thorough consideration of nanomaterial biological interactions is essential to inform risk assessments, develop targeted applications, and rationally design future nanomaterials.<sup>1,2</sup> Current regulatory requirements do not consider potential hazard from different forms of nanomaterials and the degree to which regulators can use comparable materials in a read-across approach is an ongoing area of exploration.<sup>3</sup> Understanding what physicochemical parameters drive nanomaterials' similarities and differences with respect to hazard not only helps regulators make prudent decisions, but also helps application development and material design to advance as these relationships are derived. The many stakeholders involved make the derivation of these relationships and their impacts a priority.

One material group in which the delineation between forms is often blurred is that of copper-based nanomaterials. Their production is estimated to reach 1600 tons by 2025, making them some of the most-produced nanomaterials worldwide.<sup>4,5</sup> This estimate includes both pure copper nanoparticles (Cu NPs) and various copper oxide nanoparticles (CuO NPs, Cu<sub>2</sub>O NPs, and Cu(OH)<sub>2</sub> NPs). Copper-based nanomaterials have been found to cause similar toxic effects as bulk Cu in zebrafish, which include gill dysfunction, oxidative stress, hatching delay, impaired osmoregulation, and acute lethality.<sup>6-9</sup> However, their published toxicity values vary greatly. The median lethal concentration (LC<sub>50</sub>) for Cu NPs in developing zebrafish ranges from 0.22 – 24 mg/L and CuO NPs appear to be significantly less toxic with values reported between 64 – 840 mg/L.<sup>6,9-15</sup> The wide range of the LC<sub>50</sub> values found for individual particle types may be due to differences in embryonic age, exposure duration, chorion status, water chemistry, particle size, and purity among experiments which then influence dissolution, agglomeration dynamics, and surface chemistry of the nanomaterials.<sup>16,17</sup>

Differences between Cu NP and CuO NP toxicity are more difficult to explain. Often, ionic dissolution is considered the driving mechanism between both Cu NP and CuO NP toxicity.<sup>18</sup> Cu ion release rate depends on a variety of media parameters including pH, dissolved oxygen, concentration of nanomaterial, ionic strength of the media, presence of dissolved organic matter, and types of cations and anions present.<sup>16,19,20</sup> One key difference between Cu and CuO is that the dissolution of metallic Cu can generate reactive oxygen species (ROS), while the dissolution of CuO does not.<sup>20,21</sup> ROS is known to contribute to the toxicity of many nanomaterials, but the release of ions and their resulting toxicity can make it difficult to differentiate which mechanism is dominating.

Embryonic zebrafish are a model organism often used to test for nanoparticle hazards and impacts because they develop rapidly, are easy to use and house, and most importantly, because they have conserved homology to higher-order vertebrates like humans.<sup>12,22,23</sup> This model system has been used to extrapolate experimental findings to both environmental and human health contexts. During their first 72 hours of development, zebrafish embryos possess a protective, porous chorion that can sequester metal ions and prevent them from entering the perivitelline space.<sup>12,24</sup> Removal of the chorion allows for direct exposure to the developing embryo which enables the identification of NPs that can disrupt development, interfere with molecular signaling, elicit malformations, alter behavior, or disrupt homeostasis in a whole vertebrate system.<sup>2,22,25–28</sup> Conversely, keeping the chorion intact during exposure maintains aquatic environmental relevance to piscine toxicity and consistency with results from standardized methods such as the OECD Fish Embryo Toxicity (FET) test.<sup>15,29,30</sup> For these reasons, zebrafish have become a powerful model within the field of nanotoxicology, where diverse engineering capabilities can alter suites of nanomaterial physicochemical characteristics with potentially concomitant effects on human and environmental risks.

Here, our objective was to understand the key contributors to Cu-based NP toxicity and determine the role of the chorion on the relative influence of those parameters. We selected two Cu-based NPs with the same primary particle size (<50 nm), shape (spherical), and outer surface chemistry (CuO NPs and Cu NPs coated with a 1.4 nm CuO shell) and compared their toxicity with ionic Cu as CuSO<sub>4</sub> using either chorion-intact (CI) or dechorionated (DC) embryonic zebrafish. As the Cu NPs are only covered with a thin (1.4 nm) layer of copper oxide and Cu has a higher oxidative capacity than CuO (due to differences in oxidation states), we anticipated differences in their dissolution and potential to generate ROS and hypothesized that these mechanisms would differentially influence toxicity. Our integrative approach allows us to tease apart the relative contribution of Cu ions to Cu-based NP toxicity and determine how the chorion status of the embryos may alter those mechanisms.

## Experimental

### Materials

Cu NPs with a 1.4 nm CuO shell were purchased from Alfa Aesar (Product no. 45504, lot no. D08Z052, Ward Hill, MA, USA) and CuO NPs were purchased from Sigma-Aldrich (St. Louis, MO, USA). The primary particle size of both particles was < 50 nm and no surface stabilizers, capping agents, or linkers were present on their surfaces, as reported by the manufacturers. NPs were stored dry until use per manufacturer's recommendations. Reagent-grade copper sulfate pentahydrate was purchased from Mallinckrodt Chemicals (Phillipsburg, NJ, USA).

### Exposure media

Fish water (FW) was prepared by mixing 0.26 g/L Instant Ocean salts (Aquatic Ecosystems, Apopka, FL, USA) in reverse osmosis water and adjusting the pH to  $7.2 \pm 0.2$  with sodium

bicarbonate.<sup>31</sup> Conductivity was between 480–520  $\mu\text{S}/\text{cm}$ . All experiments were conducted in FW unless otherwise indicated.

### Exposure suspensions

Dry particles were suspended in FW to create a 1000 mg Cu/L stock and sonicated for 2 minutes at 40% intensity using a VCX 750 Vibra-Cell sonicator equipped with a cup-horn style high intensity probe and recirculating water bath to maintain temperature (Sonics & Materials Inc., Newtown, CT, USA). No stabilizers were added to the exposure solutions to modify agglomeration of the bare particles. Stock solutions were made fresh for each experiment. Five-fold serial dilutions were performed in FW and were mixed by vortexing prior to making each subsequent dilution. Exposure concentrations ranged from 0–250 mg Cu/L for nanoparticle exposures and 0–10 mg Cu/L for the  $\text{CuSO}_4$  exposures. All concentrations are expressed as mass of Cu for consistency and clarity.

### NP characterization

The hydrodynamic diameter (HDD) and zeta potential (ZP) for Cu NPs and CuO NPs was measured in a 10 mg Cu/L suspension in FW at 26.9 °C using a Malvern Zetasizer Nano (Malvern Instruments Ltd, Worcestershire, UK). Two independent suspensions were each run in triplicate to obtain the average HDD, size distribution, and zeta potential measurements. Stocks were aliquoted into 1 mL samples and stored in microcentrifuge tubes at 26.9 °C. Measurements were taken once per day for five days. Samples were kept undisturbed and then briefly vortexed prior to each measurement.

### NP dissolution

NP dissolution rate in FW was measured abiotically. 10 mg Cu/L suspensions were prepared from 1000 mg Cu/L stocks as described previously. Suspensions were placed in clear 96-well plates with 200  $\mu\text{L}$  per well. At 0, 3, 24, 72, and 120 h, 180  $\mu\text{L}$  from three independent wells was collected and filtered through a 3kDa (equivalent to approximately 0.25 nm) centrifugal polyethersulfone membrane (VWR #82031-346, Radnor, PA, USA) at 8000 rpm for 10 minutes. 100  $\mu\text{L}$  of filtrate was transferred to a polystyrene tube and stored at  $-4$  °C until acidification. Samples were thawed and acidified with 70% trace-metal grade nitric acid.<sup>32</sup> Samples with a 3% nitric acid final proportion and 1  $\mu\text{g}/\text{L}$  internal indium standard with copper ICP standards (Ricca Chemical Company, Arlington, TX, USA) were analyzed for Cu by ICP-MS (Thermo Fisher Scientific, Waltham, MA, USA) in triplicate.

### Zebrafish embryo toxicity assay

Adult zebrafish (*Danio rerio*) were maintained at the Sinnhuber Aquatic Research Laboratory at Oregon State University. Embryos were collected from group spawns of wild-type 5D zebrafish and staged to ensure all embryos were in the shield stage of the gastrula period at the start of each experiment.<sup>33</sup> Embryos were separated and half were enzymatically dechorionated at 6 hours post fertilization (hpf) with pronase (Sigma Aldrich) following the protocol of Usenko et al.<sup>34</sup> At 8 hpf, embryos were individually exposed to NP suspensions or  $\text{CuSO}_4$  in FW with or without their protective chorions in clear 96-well plates (24 embryos per concentration, per chorion status). We chose our concentration-

response range so that it would include exposures that elicited no toxicity, some toxicity, and total toxicity in order to generate LC<sub>50</sub> and EC<sub>50</sub> values. Controls consisted of both chorion-intact and dechorionated embryos. Plates were covered with Parafilm to minimize evaporation and incubated at 26.9 °C under a 14:10 h light:dark photoperiod. Zebrafish embryos were observed at 24 and 120 hpf for mortality as well as developmental, morphological, and behavioural endpoints as described in Truong et al.<sup>27</sup> At 24 hpf, embryos were observed for mortality, developmental progression, notochord malformation, and presence of spontaneous movement. At 120 hpf, embryos were observed for mortality, visual malformations of the axis, brain, circulation, eyes, fins, jaw, otic vesicle, pigment, snout, somites, swim bladder, trunk, yolk sac, and pericardial space. Tactile response was evaluated by lightly agitating the embryo with a small wire tool and observing its response as compared to control embryos at 120 hpf. It was recorded in free-swimming larvae, and if hatching had not occurred, the embryo was removed from its chorion prior to evaluation. Hatching success was recorded for only chorion intact exposures. The percent frequency of each endpoint was calculated for each treatment. Representative images were taken of fish at 24 and 120 hpf on an Olympus Microscope SZX10-ILLK (Olympus Corporation, Tokyo, Japan) using Olympus cellSens software (version 1.11). All experiments were performed in compliance with national care and use guidelines as prescribed by the American Association for Laboratory Animal Science and approved by the Institutional Animal Care and Use Committee (IACUC) at Oregon State University.

#### Quantification of Cu accumulation in zebrafish embryos

Cu accumulation was determined by ICP-MS in dechorionated (DC) and chorion intact (CI) embryos in which 50% or more survivability was observed. After observation at 120 hpf, all surviving embryos were removed from the 96-well plates and gently rinsed twice with clean FW. Unhatched embryos were manually removed from their chorions prior to washing. Chorions were grouped and washed twice with clean FW before being stored at -4 °C prior to digestion. Embryos were also transferred to polystyrene tubes (no more than 6 per tube), euthanized by freezing and stored in the same way. Samples were digested by adding 3 mL of trace-metal grade nitric acid and evaporated at 200° C, repeating this process three times. Samples had a final 3% nitric acid concentration with 1 µg/L internal indium standard and were analysed for Cu by ICP-MS in triplicate.<sup>30</sup>

#### Spectrophotometric ROS quantification

The fluorescent probe dichlorofluorescein (DCF) was used to abiotically quantify ROS generation by the nanomaterials. Dichlorofluorescein diacetate (DCF-DA) was first hydrolysed to dichlorodihydrofluorescein diacetate (DCHF-DA) with 0.01 N NaOH in MQ water by incubation for 30 minutes in the dark at room temperature. Black-walled 96 well plates were prepared with six concentrations of each nanomaterial (10–125 mg Cu/L) in 0.1 X phosphate buffered saline (PBS). DCHF-DA was added to each well for a final concentration of 64 µM and a total well volume of 200 µL. The plate was read on a SpectraMax M2 Spectrophotometer (Molecular Devices, Sunnyvale, CA, USA) with an excitation wavelength of 485 nm and emission of 530 nm every five minutes for 90 minutes. Fluorescence was converted to H<sub>2</sub>O<sub>2</sub> equivalents using a standard curve of H<sub>2</sub>O<sub>2</sub> between 0–

120  $\mu\text{M}$  following the same protocol. Rate of ROS generation was determined by linear regression.

## Statistics

Sigma Plot 13.0 (Systat Software, San Jose, CA, USA) was used for the statistical tests. Three-way ANOVA was used to determine the effects of Cu exposure type, concentration, and chorion status with Holm-Sidak pairwise comparisons used when ANOVA indicated significance. Fisher's exact test was used to determine significance of embryonic zebrafish endpoint frequencies relative to control fish. All error bars represent the standard error of the mean. Concentration-response curves and  $\text{L}/\text{EC}_{50}$  values were generated using the *drc* package in R version 3.1.2.<sup>35,36</sup> Differences were considered to be statistically significant at  $p < 0.05$  for all analyses.

## Results

### Cu NP and CuO NP characterization in the exposure media

Despite their similar surfaces and primary particle sizes (<50 nm), the two particles had significantly different agglomeration behaviour over time. Over the five day experimental time frame, Cu NPs had an average HDD of  $763.0 \pm 278$  nm and CuO NPs had a significantly higher average HDD of  $2037.6 \pm 1324$  nm. The daily trends of the HDD for each NP are shown in Figure 1A, and are presented tabularly in Table S2. CuO NPs had significantly higher polydispersity than Cu NPs (Figure 1B). Cu NPs maintained the same HDD over 5 days, while CuO NPs increased in size from 1370 nm to 4100 nm after day 3. The zeta potential of both particles was similar over the experimental time frame, with a significant shift from  $-11.5$  mV to  $-8.5$  mV after day 4 (Figure 1C). The measurement of dissolved Cu by ICP-MS revealed that Cu NPs had no significant release of Cu ions over the 120 hour dissolution test. At 24 hours, Cu NPs had only dissolved by  $0.12 \pm 0.1$  % while CuO NPs dissolved over 10 times more at  $1.53 \pm 0.05$  % (Figure 2). These differences were maintained at 72 hours and 120 hours. Total dissolution of Cu NPs at 120 hours was  $0.12 \pm 0.02$  %, while CuO NP dissolution reached  $2.6 \pm 0.3$  % over the same time frame.

### Cu uptake and accumulation in embryonic zebrafish

We found that DC fish were susceptible to concentration-dependent accumulation of Cu from exposure to both Cu and CuO NPs, while no trend could be observed in CI fish (Figure 3).  $\text{CuSO}_4$  exposure did not result in any significant increase in Cu accumulation in surviving embryos relative to control whether embryos were dechorionated or intact during the exposure.

Nonlethal concentrations of Cu exposure induced hatching delay, allowing measurement of Cu accumulation on the chorions of CI fish at 120 hpf to compare to DC embryos (Figure 4). There was a significant difference in the affinity of Cu for chorionic membranes versus the DC fish embryos. When comparing between the chorion alone from CI exposures and the dechorionated fish from DC exposures, the chorion was able to sequester 10 fold more Cu by weight in comparison to DC fish embryos. The exposure concentration 10 mg Cu/L CuO NPs had  $0.18 \pm 0.01$   $\mu\text{g}$  Cu/fish compared to  $2.4$   $\mu\text{g}$  Cu/chorion. The same CI fish exposed

to 10 mg Cu/L had a measured Cu content of  $0.028 \pm 0.004 \mu\text{g}/\text{fish}$  which was not statistically different from control fish Cu content ( $0.0099 \pm 0.0006 \mu\text{g Cu}/\text{fish}$ ).

### Toxicity to embryonic zebrafish

In DC exposures, Cu NPs and  $\text{CuSO}_4$  caused total mortality at concentrations above 10 and 2 mg Cu/L, respectively, while CuO NP exposure only resulted in partial mortality at equivalent exposures (Figure 5). Calculated concentrations at which exposure caused 50% lethality ( $\text{LC}_{50}$ ) and concentration response curves revealed  $\text{CuSO}_4$  as the most toxic source of Cu on a mass basis, followed by Cu NPs and CuO NPs (Table 1). We observed a similar trend in CI exposures, though all toxicity was significantly diminished from DC exposures, by as much as 400% in both Cu NP and  $\text{CuSO}_4$  exposures. Comparing 24 hpf and 120 hpf  $\text{LC}_{50}$  values revealed that Cu NPs were the only Cu source to increase toxicity with increased exposure time, and only in CI exposures.

Observed sublethal impacts in both DC and CI exposures were abnormal tactile response (ATR), yolk sac edema (YSE), axis, and trunk malformations, with the additional endpoint of hatching delay in CI exposures (Figure S1, S2). DC embryos were most sensitive to  $\text{CuSO}_4$  for both ATR and YSE with LOAELs of 0.2 and 0.048 mg Cu/L, respectively, and were least sensitive to Cu NPs (LOAELs of 0.4 and 2 mg Cu/L, respectively). CI fish were more susceptible to YSE than DC fish, while the opposite was true for ATR. However, it is likely that both endpoints were exacerbated by hatching delay (Figure S1), making YSE more likely due to compression in the chorion and ATR difficult to assess as the chorion impedes movement.  $\text{CuSO}_4$  elicited the strongest hatching delay response ( $\text{EC}_{50}$   $0.30 \pm 0.04$  mg Cu/L), followed by CuO NPs ( $\text{EC}_{50}$   $0.6 \pm 0.2$  mg Cu/L) and then Cu NPs ( $\text{EC}_{50}$   $1.2 \pm 0.2$  mg Cu/L).

### ROS generation and toxicity correlation

The EZ Metric is a combined measure of both morbidity and mortality, developed specifically for use in developing embryonic zebrafish toxicity assessment.<sup>23</sup> The weighted score assigns a value to each toxicity endpoint observed which is weighted by their overall impact on survival, giving each exposure a score between 0 (no effect) and 1 (maximum effect). We performed a Pearson correlation between the weighted EZ Metric score (Figure S3) elicited by each nanomaterial type and the potential for ROS generation reported as concentration equivalent  $\text{H}_2\text{O}_2$  produced. Figure 7 clearly shows the strong positive correlation between ROS generation and EZ Metric score ( $r = 0.91$ ,  $p = 0.01$ ) for Cu NPs and no correlation ( $r = -0.41$ ,  $p = 0.18$ ) for CuO NPs. The concentrations at which Cu NPs elicited toxicity were much lower than those tested in the ROS assay, likely due to the difference in media used and the abiotic nature of the assay.

### Discussion

Though Cu and CuO have fundamentally different oxidative capacities, dissolution kinetics, and elemental composition, information on their nanomaterial forms are often considered together when assessing hazard. Typically, the parameters of agglomerate size, zeta potential, and dissolution are used to explain their toxicity because they are relatively simple

to experimentally determine. We hypothesized that it is the capacity for ROS generation that drives the difference between Cu NP and CuO NP toxicity, which we evaluated through a simple functional assay. The use of functional assays to identify likely parameters that drive nanomaterial toxicity can provide important mechanistic clues for researchers and regulators without the time, expense, or animals required for more in-depth studies.

We evaluated the agglomerate behavior, zeta potential, dissolution, ROS generation, and organismal uptake of Cu NPs and CuO NPs and correlated these data to lethal and sublethal toxicity responses in CI and DC embryonic zebrafish at a neutral pH with a five day exposure duration. We found that only the ROS generation of Cu NPs adequately explained the toxicity we observed (Figure 7). Previous work has demonstrated oxidative stress responses from Cu NP or CuO NP exposure, but it is often unclear whether the observed toxicity is derived from released ionic species or nanomaterial exposure.<sup>9,18,37-39</sup> Others have suggested a Cu-based NP-specific effect based on the Trojan horse mechanism, in which whole NPs are taken up by the organism and endocytotic transport to acidic compartments (i.e. lysosomes) causes release of toxic ions directly into the cytoplasm.<sup>40</sup> In the presence of oxygen, Cu NPs can form superoxide and hydrogen peroxide in addition to releasing Cu ions.<sup>21,41</sup> These reactions do not occur to the same extent with CuO NPs, as CuO dissolution proceeds by hydrolysis to form various Cu hydroxyl complexes.<sup>42</sup> Based on this finding, we propose that it is the ability of Cu NPs to generate ROS, rather than their dissolution or another nano-specific mechanism, that makes them more toxic than CuO NPs. We propose evaluation of surface stabilizers and capping agents on the redox potential and ROS species produced by Cu-based nanomaterials as the next steps towards mechanistic understanding of Cu-based nanomaterial toxicity.

The only case in which another measured parameter aligned with biological impacts was that of hatching interference (Figure S1). The magnitude of hatching interference by each Cu exposure followed the same trend we would expect based on our dissolution results, with soluble Cu eliciting the strongest inhibition, followed by CuO NPs, and then Cu NPs. Both NPs had low measured dissolution, likely due to their high agglomerate sizes in addition to the neutral pH of the exposure media. Due to the known relationship between Cu ion exposure and hatching delay, we assume that hatching interference was primarily driven by the presence of Cu ion in our exposure media. The Cu ion inhibits ZHE1 by binding the zinc core within the enzyme and deactivating it, which a NP would not be able to do directly due to its large relative size. Additionally, the LOAELs for ATR and YSE suggest that the zebrafish are more sensitive to the sublethal effects of CuO NPs than Cu NPs, which are both known to be caused by soluble Cu in addition to copper-based nanomaterial exposure. This is strong evidence that, even in the presence of the embryo, the dissolution trend we observed of CuO NPs dissolving to a greater extent than Cu NPs holds true in our exposures. It is possible that the presence of the embryo in the exposure solution altered the dissolution of the NPs or complexation with dissolved organic matter contributed to a transformation of the dissolved Cu to non-bioavailable species. However, 7.8 ppm of humic acid was required to rescue hatching interference to embryonic zebrafish by Cu NPs, making it unlikely that a small contribution of organic matter from the presence of the zebrafish embryo is enough to rescue a lethal response in our scenario.<sup>43</sup>



We evaluated both CI and DC embryonic zebrafish to maintain aquatic environmental relevance and allow us to extrapolate our derived nanomaterial-biological interactions to broader vertebrate contexts. We found that the chorionic membrane mediated toxicity of both Cu NPs and CuO NPs up to one order of magnitude. The chorion completely prevented Cu uptake in all CI exposures, which was significant and concentration-dependent in DC zebrafish, likely due to its ability to sequester Cu and protect the embryo from direct exposure until hatching.<sup>12</sup> Additionally, the chorion sorbed up to 100% of the CuO present in CuO NP exposures, and over 15% of the Cu present on Cu NP exposures. This sorption could have been from NP agglomeration causing their sedimentation out of the water column, or a high affinity to the chorion, as some evidence suggests that CuO NPs have a high affinity for biotic substrates.<sup>32</sup> Therefore, embryonic zebrafish studies designed to inform risks to other organisms that do not possess a protective chorion, such as humans or other mammals, may be severely underestimating the risks of nanomaterials and missing potential effects and novel interactions due to a lack of dose directly to the embryo. Further, our DC LC<sub>50</sub> value was very similar to other published LC<sub>50</sub> values for Cu nanomaterials exposed to hatched, larval zebrafish, which suggests that DC zebrafish can provide just as much information as larval exposures, and provides evidence that hazard assessments done on chorion-intact fish, such as the recently established FET, should be interpreted solely for environmental risks and may not be adequately evaluating the all vertebrate hazards presented by nanomaterials.<sup>6,13–15,29,44</sup>

## Conclusions

While embryonic zebrafish toxicity was not correlated with agglomeration size, ZP, or dissolution, we demonstrated a strong correlation between toxicity and nanomaterial ROS generation potential. We suggest the assessment of a nanomaterial's ability to generate ROS become a common parameter evaluated when determining nanotoxicity and its mechanisms. The assay used here can provide quick data to inform nanomaterial hazard while being simple and cost effective to perform. In addition, we offer evidence that the chorionic status of zebrafish embryos can significantly alter their exposure to nanomaterials, making it an important consideration in nanotoxicological experimental design.

## Supplementary Material

Refer to Web version on PubMed Central for supplementary material.

## Acknowledgments

This work is funded by grants from the National Science Foundation (NSF Grant # 1438165), the National Institutes of Health (award number ES017552), a National Institute of Environmental Health Sciences Training Grant (T32 ES007060), and an Environmental Health Sciences Core Center grant (P30 ES000210). The authors would like to thank the Sinnhuber Aquatic Research Laboratory (SARL) at Oregon State University for providing the zebrafish embryos.

## References

1. Harper S, Usenko C, Hutchison J, Maddux B, Tanguay R. In vivo biodistribution and toxicity depends on nanomaterial composition, size, surface functionalisation and route of exposure. *Journal of Experimental Nanoscience*. 2008; 3:195–206.

2. Harper SL, Carriere JL, Miller JM, Hutchison JE, Maddux BLS, Tanguay RL. Systematic evaluation of nanomaterial toxicity: Utility of standardized materials and rapid assays. *ACS Nano*. 2011; 5:4688–4697. [PubMed: 21609003]
3. Mattsson MO, Simkó M. The changing face of nanomaterials: Risk assessment challenges along the value chain. *Regulatory Toxicology and Pharmacology*. 2017; 84:105–115. [PubMed: 27998719]
4. Hou J, Wang X, Hayat T, Wang X. Ecotoxicological effects and mechanism of CuO nanoparticles to individual organisms. *Environmental Pollution*. 2017; 221:209–217. [PubMed: 27939631]
5. Keller AA, McFerran S, Lazareva A, Suh S. Global life cycle releases of engineered nanomaterials. *Journal of Nanoparticle Research*. 2013; 15:1692.
6. Griffith RJ, Weil R, Hyndman KA, Denslow ND, Powers K, Taylor D, Barber DS. Exposure to copper nanoparticles causes gill injury and acute lethality in zebrafish (*Danio rerio*). *Environmental Science and Technology*. 2007; 41:8178–8186. [PubMed: 18186356]
7. Lin S, Zhao Y, Ji Z, Ear J, Chang CH, Zhang H, Low-Kam C, Yamada K, Meng H, Wang X, Liu R, Pokhrel S, Mädler L, Damoiseaux R, Xia T, Godwin HA, Lin S, Nel AE. Zebrafish high-throughput screening to study the impact of dissolvable metal oxide nanoparticles on the hatching enzyme, ZHE1. *Small*. 2013; 9:1776–1785. [PubMed: 23180726]
8. Muller EB, Lin S, Nisbet RM. Quantitative Adverse Outcome Pathway Analysis of Hatching in Zebrafish with CuO Nanoparticles. *Environmental Science and Technology*. 2015; 49:11817–11824. [PubMed: 26378804]
9. Ganesan S, Anaimalai Thirumurthi N, Raghunath A, Vijayakumar S, Perumal E. Acute and sub-lethal exposure to copper oxide nanoparticles causes oxidative stress and teratogenicity in zebrafish embryos. *Journal of Applied Toxicology*. 2016; 36:554–567. [PubMed: 26493272]
10. Heinlaan M, Muna M, Knöbel M, Kistler D, Odzak N, Kühnel D, Müller J, Gupta GS, Kumar A, Shanker R, Sigg L. Natural water as the test medium for Ag and CuO nanoparticle hazard evaluation: An interlaboratory case study. *Environmental Pollution*. 2016; 216:689–699. [PubMed: 27357482]
11. Kovřížnych JA, Sotníková R, Zeljenková D, Rollerová E, Szabová E, Wimmerová S. Acute toxicity of 31 different nanoparticles to zebrafish (*Danio rerio*) tested in adulthood and in early life stages – comparative study. *Interdisciplinary Toxicology*. 2013; 6:67–73. [PubMed: 24179431]
12. Lin S, Zhao Y, Xia T, Meng H, Ji Z, Liu R, George S, Xiong S, Wang X, Zhang H, Pokhrel S, Mädler L, Damoiseaux R, Lin S, Nel AE. High content screening in zebrafish speeds up hazard ranking of transition metal oxide nanoparticles. *ACS Nano*. 2011; 5:7284–7295. [PubMed: 21851096]
13. Bai W, Tian W, Zhang Z, He X, Ma Y, Liu N, Chai Z. Effects of copper nanoparticles on the development of zebrafish embryos. *Journal of nanoscience and nanotechnology*. 2010; 10:8670–6. [PubMed: 21121381]
14. Hua J, Vijver MG, Ahmad F, Richardson MK, Peijnenburg WJGM. Toxicity of different-sized copper nano- and submicron particles and their shed copper ions to zebrafish embryos. *Environmental Toxicology and Chemistry*. 2014; 33:1774–1782. [PubMed: 24839162]
15. Song L, Vijver MG, Peijnenburg WJ, Galloway TS, Tyler CR. A comparative analysis on the in vivo toxicity of copper nanoparticles in three species of freshwater fish. *Chemosphere*. 2015; 139:181–189. [PubMed: 26121603]
16. Conway JR, Adeleye AS, Gardea-Torresdey J, Keller AA. Aggregation, dissolution, and transformation of copper nanoparticles in natural waters. *Environmental Science and Technology*. 2015; 49:2749–2756. [PubMed: 25664878]
17. Keller AA, Adeleye AS, Conway JR, Garner KL, Zhao L, Cherr GN, Hong J, Gardea-Torresdey JL, Godwin HA, Hanna S, Ji Z, Kaweeteerawat C, Lin S, Lenihan HS, Miller RJ, Nel AE, Peralta-Videa JR, Walker SL, Taylor AA, Torres-Duarte C, Zink JJ, Zuverza-Mena N. Comparative environmental fate and toxicity of copper nanomaterials. *NanoImpact*. 2017; 7:28–40.
18. Misra SK, Nuseibeh S, Dybowska A, Berhanu D, Tetley TD, Valsami-Jones E. Comparative study using spheres, rods and spindle-shaped nanoplatelets on dispersion stability, dissolution and toxicity of CuO nanomaterials. *Nanotoxicology*. 2014; 8:422–432. [PubMed: 23590525]
19. Jiang C, Castellon BT, Matson CW, Aiken GR, Hsu-Kim H. Relative Contributions of Copper Oxide Nanoparticles and Dissolved Copper to Cu Uptake Kinetics of Gulf Killifish (*Fundulus*

- grandis) Embryos. *Environmental Science and Technology*. 2017; 51:1395–1404. [PubMed: 28081364]
20. Palmer DA, Bénézeth P. 14th International Conference on the Properties of Water and Steam in Kyoto; 2008; 491–496.
  21. Olszowka SA, Manning MA, Barkatt A. Copper Dissolution and Hydrogen Peroxide Formation in Aqueous Media. *CORROSION*. 1992; 48:411–418.
  22. Lin S, Lin S, Zhao Y, Nel AE. Zebrafish: An in vivo model for nano EHS studies. *Small*. 2013; 9:1608–1618. [PubMed: 23208995]
  23. Harper B, Thomas D, Chikkagoudar S, Baker N, Tang K, Heredia-Langner A, Lins R, Harper S. Comparative hazard analysis and toxicological modeling of diverse nanomaterials using the embryonic zebrafish (EZ) metric of toxicity. *Journal of Nanoparticle Research*. 2015; 17:1–12.
  24. Rawson DM, Zhang T, Kalicharan D, Jongebloed WL. Field emission scanning electron microscopy and transmission electron microscopy studies of the chorion, plasma membrane and syncytial layers of the gastrula-stage embryo of the zebrafish *Brachydanio rerio*: A consideration of the structural and functional. *Aquaculture Research*. 2000; 31:325–336.
  25. Harper B, Sinche F, Wu R, Gowrishankar M, Marquart G, Mackiewicz M, Harper S. The Impact of Surface Ligands and Synthesis Method on the Toxicity of Glutathione-Coated Gold Nanoparticles. *Nanomaterials*. 2014; 4:355–371. [PubMed: 26213631]
  26. Harper BJ, Clendaniel A, Sinche F, Way D, Hughes M, Schardt J, Simonsen J, Stefaniak AB, Harper SL. Impacts of chemical modification on the toxicity of diverse nanocellulose materials to developing zebrafish. *Cellulose*. 2016; 23:1763–1775. [PubMed: 27468180]
  27. Truong L, Harper SL, Tanguay RL. *Drug Safety Evaluation*. Vol. 691. Humana Press; Totowa: 2011. 271–279.
  28. Truong L, Saili KS, Miller JM, Hutchison JE, Tanguay RL. Persistent adult zebrafish behavioral deficits results from acute embryonic exposure to gold nanoparticles. *Comparative Biochemistry and Physiology - C Toxicology and Pharmacology*. 2012; 155:269–274. [PubMed: 21946249]
  29. OECD. Test No. 236: Fish Embryo Acute Toxicity (FET) Test. 2013.
  30. Wu F, Harper BJ, Harper SL. Differential dissolution and toxicity of surface functionalized silver nanoparticles in small-scale microcosms: impacts of community complexity. *Environmental Science: Nano*. 2017; 4:359–372.
  31. Bonventre JA, Pryor JB, Harper BJ, Harper SL. The impact of aminated surface ligands and silica shells on the stability, uptake, and toxicity of engineered silver nanoparticles. *Journal of Nanoparticle Research*. 2014; 16:2761. [PubMed: 25484618]
  32. Wu F, Bortvedt A, Harper BJ, Crandon LE, Harper SL. Uptake and toxicity of CuO nanoparticles to *Daphnia magna* varies between indirect dietary and direct waterborne exposures. *Aquatic Toxicology*. 2017; 190:78–86. [PubMed: 28697458]
  33. Kimmel CB, Ballard WW, Kimmel SR, Ullmann B, Schilling TF. Stages of embryonic development of the zebrafish. *Developmental dynamics*. 1995; 203:253–310. [PubMed: 8589427]
  34. Usenko CY, Harper SL, Tanguay RL. Fullerene C60 exposure elicits an oxidative stress response in embryonic zebrafish. *Toxicology and Applied Pharmacology*. 2008; 229:44–55. [PubMed: 18299140]
  35. Ritz C, Baty F, Streibig J. Dose-Response Analysis Using R. *PLOS ONE*. 2015; 10:e0146021. [PubMed: 26717316]
  36. R Core Team. *R: A language and environment for statistical computing*. 2016
  37. Leite CE, Maboni LdO, Cruz FF, Rosemberg DB, Zimmermann FF, Pereira TCB, Bogo MR, Bonan CD, Campos MM, Morrone FB, Battastini AMO. Involvement of purinergic system in inflammation and toxicity induced by copper in zebrafish larvae. *Toxicology and Applied Pharmacology*. 2013; 272:681–689. [PubMed: 23933163]
  38. Haverroth GMB, Welang C, Mocelin RN, Postay D, Bertoncello KT, Franscescon F, Rosemberg DB, Dal Magro J, Dalla Corte CL. Copper acutely impairs behavioral function and muscle acetylcholinesterase activity in zebrafish (*Danio rerio*). *Ecotoxicology and Environmental Safety*. 2015; 122:440–447. [PubMed: 26386335]
  39. Kaweeteerawat C, Chang CH, Roy KR, Liu R, Li R, Toso D, Fischer H, Ivask A, Ji Z, Zink JI, Zhou ZH, Chanfreau GF, Telesca D, Cohen Y, Holden PA, Nel AE, Godwin HA. Cu Nanoparticles

- Have Different Impacts in *Escherichia coli* and *Lactobacillus brevis* than Their Microsized and Ionic Analogues. *ACS Nano*. 2015; 9:7215–7225. [PubMed: 26168153]
40. Studer AM, Limbach LK, Van Duc L, Krumeich F, Athanassiou EK, Gerber LC, Moch H, Stark WJ. Nanoparticle cytotoxicity depends on intracellular solubility: Comparison of stabilized copper metal and degradable copper oxide nanoparticles. *Toxicology Letters*. 2010; 197:169–174. [PubMed: 20621582]
  41. Pham AN, Xing G, Miller CJ, Waite TD. Fenton-like copper redox chemistry revisited: Hydrogen peroxide and superoxide mediation of copper-catalyzed oxidant production. *Journal of Catalysis*. 2013; 301:54–64.
  42. Plyasunova NV, Wang M, Zhang Y, Muhammed M. Critical evaluation of thermodynamics of complex formation of metal ions in aqueous solutions II. Hydrolysis and hydroxo-complexes of  $\text{Cu}^{2+}$  at 298.15 K. *Hydrometallurgy*. 1997; 45:37–51.
  43. Lin S, Taylor AA, Ji Z, Chang CH, Kinsinger NM, Ueng W, Walker SL, Nel AE. Understanding the transformation, speciation, and hazard potential of copper particles in a model septic tank system using zebrafish to monitor the effluent. *ACS Nano*. 2015; 9:2038–2048. [PubMed: 25625504]
  44. Chen D, Zhang D, Yu JC, Chan KM. Effects of  $\text{Cu}_2\text{O}$  nanoparticle and  $\text{CuCl}_2$  on zebrafish larvae and a liver cell-line. *Aquatic Toxicology*. 2011; 105:344–354. [PubMed: 21839701]

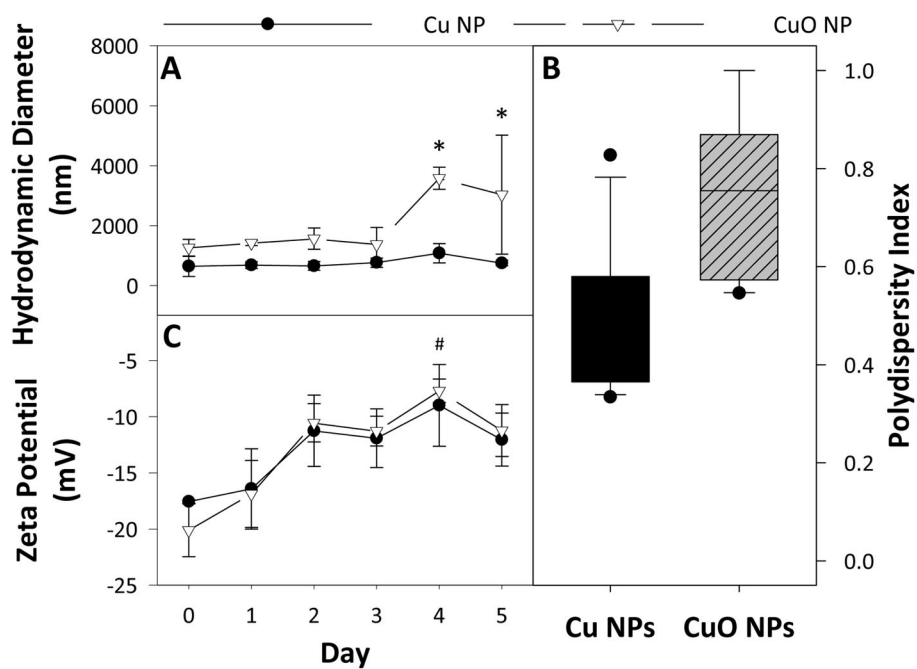


**Fig. 1.** Nanomaterial characterization by dynamic light scattering showing the average HDD (A), and the average polydispersity (B), and the average zeta potential (C) of each nanomaterial over 5 days in FW. ( ) indicates statistical difference between particle types and (#) indicates statistical difference from day 0. Error bars represent standard error of the mean and significance was determined when  $p < 0.05$ .

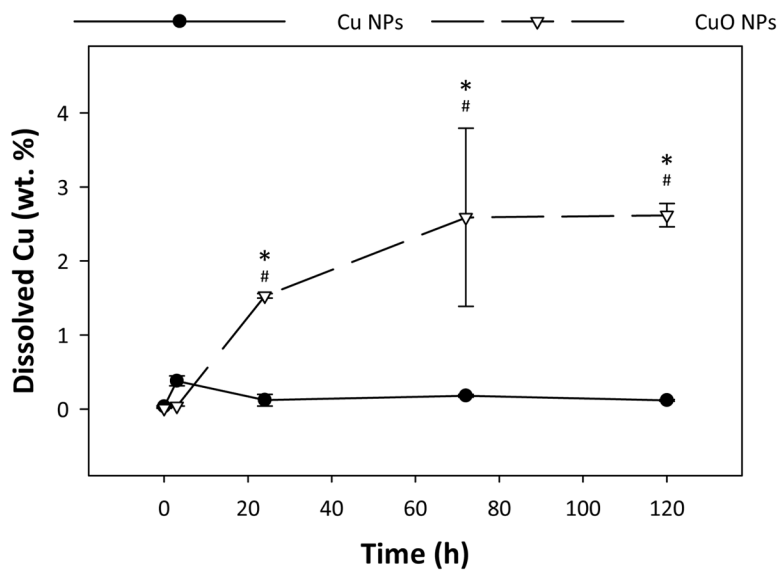


**Fig. 2.** Abiotic dissolution of Cu NPs and CuO NPs in FW measured over 120 hours by ICP-MS. ( ) indicates statistical difference between particle types. (#) indicates statistical difference from 0 hour and 3 hour time points. Error bars represent standard error of the mean and significance was determined when  $p < 0.05$ .

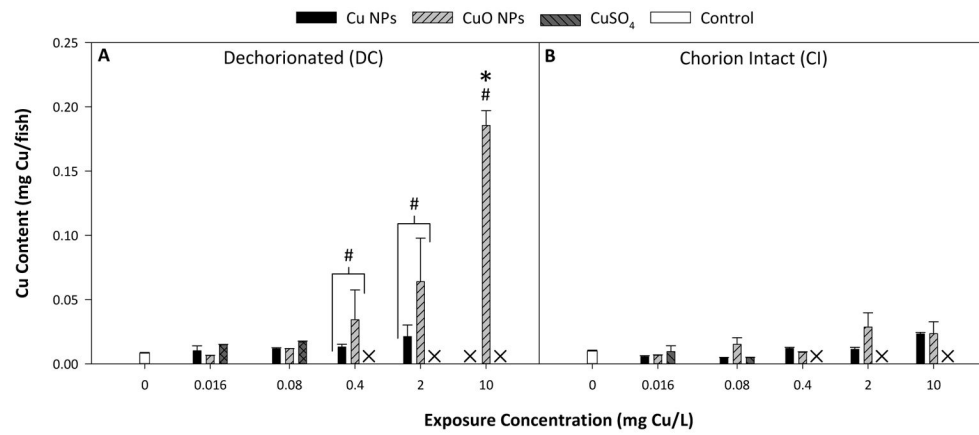


**Fig. 3.** Measured Cu accumulation in DC fish (A) and CI fish with chorions removed (B) at 120 hpf. (#) represents statistical difference between particle types. (X) indicates no data was collected due to mortality in exposed fish. (.) represents statistical difference from control. Error bars represent standard error of the mean and significance was determined when  $p < 0.05$ .

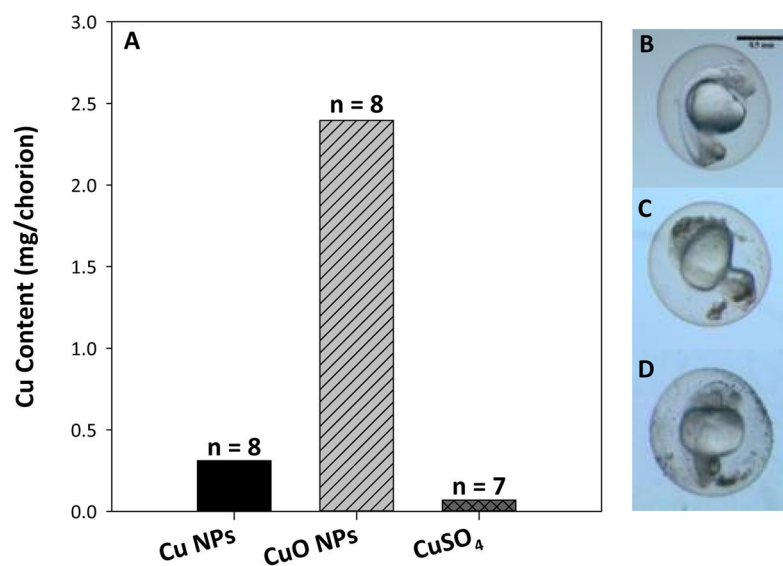


**Fig. 4.** Cu content in chorions from 120 hpf zebrafish exposed to 10 mg Cu/L from each nanoparticle type at 8 hpf or 0.4 mg Cu/L CuSO<sub>4</sub> (A) with representative images of control (B), 50 mg Cu/L Cu NP (C), and 50 mg Cu/L CuO NP (D) exposed 24 hpf zebrafish in their chorions showing visible particulate deposition. No standard error is included due to the fragility of the chorions causing breakage, requiring combination of all replicates to ensure proper accounting. Scale bar represents 0.5 mm.



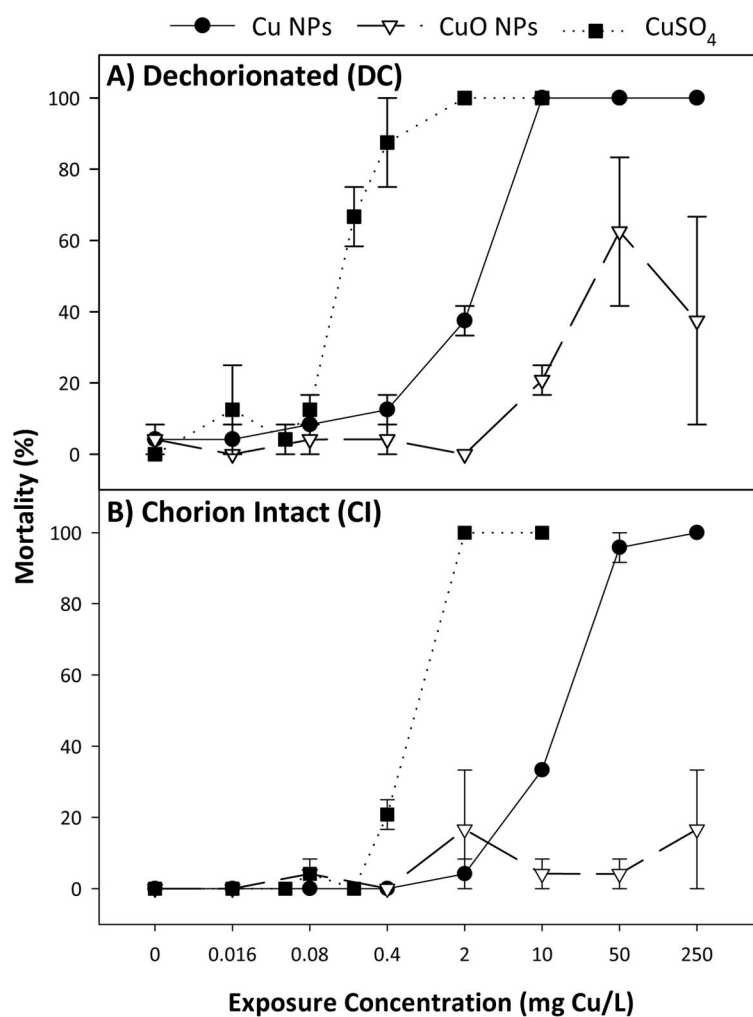


**Fig. 5.** Concentration-response curves of DC (A) and CI (B) zebrafish exposed to Cu NPs, CuO NPs, and CuSO<sub>4</sub> calculated from total mortality at 120 hpf. Error bars represent standard error of the mean.

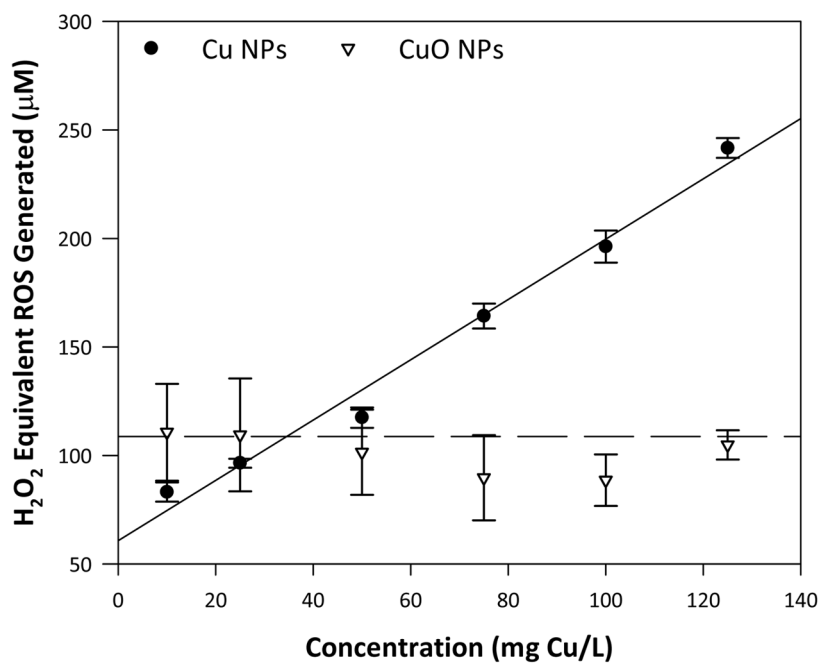


**Fig. 6.** ROS generation elicited by Cu NPs and CuO NPs (expressed as H<sub>2</sub>O<sub>2</sub> equivalents) measured over 90 minutes using a modified dichlorofluorescein assay. ROS generation as a function of concentration was modeled by simple linear regression. Error bars represent standard error of the mean.

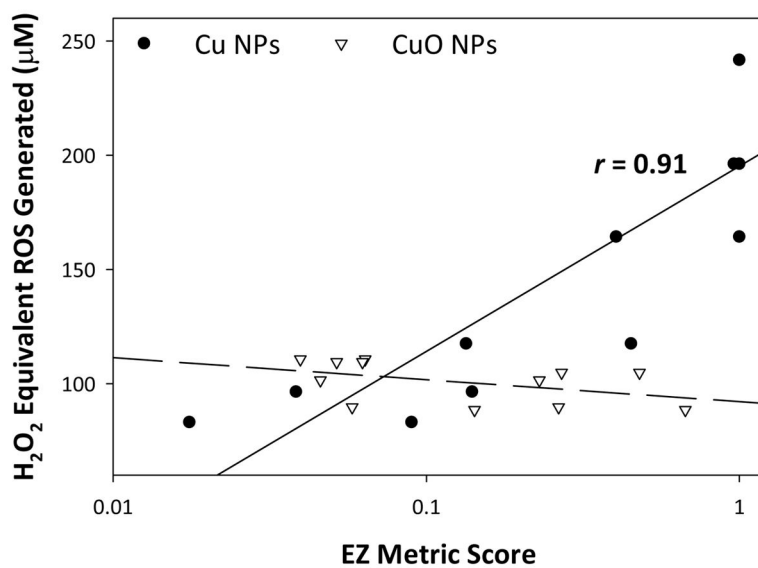


**Fig. 7.** Pearson correlation between calculated equivalent ROS generated by nanomaterials and EZ Metric scores.

Calculated LC/EC<sub>50</sub> and extrapolated LOAEL values for significant endpoints observed in zebrafish. All values are reported in units of mg Cu/L.

**Table 1**

	Cu NPs		CuO NPs		CuSO <sub>4</sub>	
	DC	CI	DC	CI	DC	CI
LC <sub>50</sub>						
24 hpf	2.7 ± 0.9	18 ± 2	> 250	> 250	0.16 ± 0.01	0.6 ± 0.1
120 hpf	2.5 ± 0.3	13.7 ± 0.8	> 250	> 250	0.016 ± 0.02	0.5 ± 0.1
120 hpf LOAEL						
Yolk sac edema	2	2	2	0.4	0.2	0.2
Tactile response	0.4	0.4	0.08	> 250	0.048	> 250
120 hpf EC50						
Hatching Delay	—	1.2 ± 0.2	—	0.6 ± 0.2	—	0.030 ± 0.04